ELSEVIER

Calculated photon echo signals for the aqueous solvated electron. The origin of ultrafast electronic dephasing

Sandra J. Rosenthal [a], Benjamin J. Schwartz [b], Peter J. Rossky [b]

[a] *Department of Chemistry and Lawrence Berkeley Laboratory, The University of California, Berkeley, CA 94720, USA*
[b] *Department of Chemistry and Biochemistry, The University of Texas, Austin, TX 78712, USA*

Abstract

Photon echo and resonant transient grating signals are calculated for the hydrated electron based on the results of quantum molecular dynamics simulations. The echo decays in $\leqslant 15$ fs. Comparison to echo calculations for organic probes and different solvent response functions reveals the origin of this ultrafast dephasing. For the strongly coupled hydrated electron, small changes in solvent configuration lead to large fluctuations in the transition frequency causing a rapid loss of electronic coherence, even in the absence of fast inertial solvent motions. In such strongly coupled systems where the echo decay is insensitive to solvation dynamics, the resonant transient grating experiment can provide a measure of the solvent response.

Photon echo measurements of organic dye molecules in liquids have been used to study both slow (static) and fast (dynamic) solvent–solute interactions [1–5]. In the limit of large inhomogeneous broadening [1] the photon echo technique eliminates contributions from different 'static' solvent configurations, allowing the characterization of fast solvent fluctuations and the degree of homogeneous line broadening in the linear absorption spectrum [7]. A theoretical formalism describing a variety of nonlinear spectroscopies including the photon echo has been developed by Loring, Yan, and Mukamel [8–12]. The time dependence of the fluctuations in the transition frequency of the chromophore arising from solvent motion, $\Delta\omega(t)$, is characterized by the solvent correlation function,

---

[1] Cho and Fleming have shown that when the broadening is not dominated by inhomogeneity a fifth-order echo experiment is required to disentangle the homogeneous dynamics [6].

$$M(t) = \frac{\langle \Delta\omega(0)\Delta\omega(t) \rangle}{\langle [\Delta\omega(0)]^2 \rangle}. \tag{1}$$

In the limit of linear response the correlation function $M(t)$ is equivalent to the nonequilibrium solvent response function, $C(t)$, which can be determined experimentally by time-resolved fluorescence measurements [13,14],

$$C(t) = \frac{\omega(t) - \omega(\infty)}{\omega(0) - \omega(\infty)}. \tag{2}$$

Here $\omega(t)$ is a characteristic frequency of the time-resolved emission spectrum. Shemetulskis and Loring [15] have calculated two-pulse photon echo signals from both nonequilibrium and equilibrium molecular dynamic simulations and found the results to be identical. This demonstrates that $C(t)$ (the nonequilibrium response) describes the solvent fluctuations for both the time period when the system evolves during an electronic coherence (the time between the first and second pulse) and during a population state

(the time period between the second and third pulse in a three pulse echo experiment). We emphasize that, therefore, $M(t)$ is equivalent to $C(t)$ for calculating photon echo signals in the linear response limit. In the Mukamel formalism for calculating the third-order polarization, the solvent dynamics are contained entirely in the lineshape function [12,16],

$$g(t) = i\lambda \int_0^t dt_1 \, M(t_1)$$

$$+ \langle [\Delta\omega]^2 \rangle \int_0^t dt_1 \int_0^{t_1} dt_2 \, M(t_2), \qquad (3)$$

where λ is the reorganization energy (the Stokes shift divided by 2) and $\langle [\Delta\omega^2] \rangle$ (the mean-square amplitude of the solvent fluctuations) is a measure of the coupling between the electronic transition frequency and a given solvent configuration. At high temperatures, these two quantities are related by the fluctuation–dissipation theorem [12],

$$\langle [\Delta\omega]^2 \rangle = 2\lambda kT. \qquad (4)$$

Hence, nonlinear optical measurements can be used to ascertain the nature of the solvent response function.

In this Letter, we solve the lineshape function for the now standard non-Markovian solvent response function which includes inertial solvent motion and apply the results to calculate photon echo signals for the aqueous electron using input parameters determined by the nonadiabatic molecular dynamic simulations of Schwartz and Rossky [17–19]. We find the interesting result that the decay of the electronic coherence is not dominated by the ultrafast time scale of inertial solvent motion in water, but is instead controlled by the enormous solvent–solute coupling in this system. We also demonstrate that resonant transient grating spectroscopy, a three pulse experiment in which the time delay between the first two pulses is zero, can be used to study inertial solvation dynamics with extremely high time resolution.

The calculated nonequilibrium solvent response function for the hydrated electron [19], displayed in Fig. 1, contains an ultrafast Gaussian inertial component. The existence of this inertial contribution to the solvent response of acetonitrile [20,21], metha-
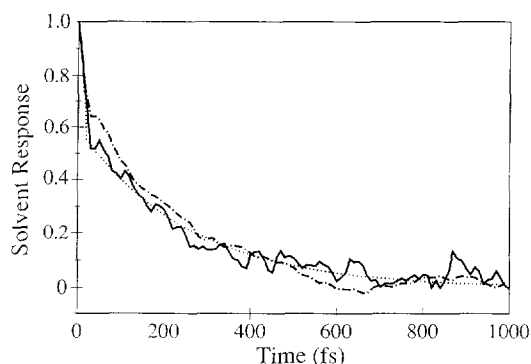

Fig. 1. The equilibrium and nonequilibrium solvent response functions for the aqueous electron and fitted result for a truncated Gaussian with an exponential tail (Eq. (5)). The parameters describing $C(t)$ with Eq. (5) are $a=0.4$, $\tau_g=20$ fs, $b=0.6$, $\tau_{exp}=250$ fs. (——) $C(t)$; (---) $M(t)$; (···) fit.

nol [21,22], and quite recently water [23], has been experimentally verified by time resolved fluorescence experiments which used large organic molecules as solvent probes. That the early time behavior of $C(t)$ can be described by a simple Gaussian was first recognized by Hynes and co-workers [24–27] and Maroncelli and Fleming [13,14]. It is common to represent the inertial portion of the solvent dynamics by expanding the Gaussian part of the solvent response at short times to $1 - t^2/\tau_g^2$ [6,16,24–28].

When the inertial solvent response function is expressed as this truncated Gaussian for short times plus an exponential term in order to describe the long time dynamics as

$$M(t) = a(1 - t^2/\tau_g^2) + b \exp(-t/\tau_{exp}), \quad t < \tau_g$$

$$M(t) = b \exp(-t/\tau_{exp}), \quad t \geqslant \tau_g, \qquad (5)$$

the lineshape function, $g(t)$, can be evaluated analytically. We find

$$g(t) = i\lambda \{ at(1 - t^2/3\tau_g^2)$$

$$+ b\tau_{exp}[1 - \exp(-t/\tau_{exp})] \}$$

$$+ \langle \Delta\omega^2 \rangle (a(t^2/2)(1 - t^2/6\tau_g^2)$$

$$+ b\tau_{exp}\{t + \tau_{exp}[\exp(-t/\tau_{exp}) - 1]\}),$$

$$t < \tau_g,$$

$$g(t) = i\lambda\{\tfrac{2}{3}a\tau_g + b\tau_{exp}[1 - \exp(-t/\tau_{exp})]\}$$

$$+ \langle \Delta\omega^2 \rangle (\tfrac{5}{12}a\tau_g^2 + b\tau_{exp}$$

$$\times \{\tau_g + \tau_{exp}[\exp(-\tau_g/\tau_{exp}) - 1]\}$$

$$+ (\tfrac{2}{3}a\tau_g + b\tau_{exp})(t - \tau_g)$$

$$+ b\tau_{exp}^2[\exp(-t/\tau_{exp}) - \exp(-\tau_g/\tau_{exp})]),$$

$$t \geqslant \tau_g. \tag{6}$$

For the hydrated electron, we find that the amplitude and time constants which describe $C(t)$ (via Eq. (5)) are $a = 0.4$, $\tau_g = 20$ fs, $b = 0.6$ and $\tau_{exp} = 250$ fs. This result is shown as the dotted line through $C(t)$ in Fig. 1. The dashed line in Fig. 1 is the equilibrium response function ($M(t)$, Eq. (1)), which is nearly identical to the nonequilibrium result ($C(t)$, Eq. (2)), indicating that solvation of the electron occurs in the linear response regime. Using the fractional Stokes shift of 0.75 computed in MD simulations [19] corresponding to a 780 nm excitation wavelength experimentally, the experimental Stokes shift is deduced to be 9660 cm^{-1}. The fluctuation–dissipation theorem (Eq. (4)) predicts a coupling strength of 1414 cm^{-1} for this Stokes shift, in good agreement with the value determined directly as the standard deviation of the fluctuating energy gap from ground state MD simulations [19].

Thus, both the magnitude and dynamics of the solvent response are within the linear regime and it is valid to use the nonequilibrium response, $C(t)$, in Eq. (3) to calculate the lineshape function.

The only remaining input required to calculate the third-order polarization is the width of the inhomogeneous distribution of solvent sites [12]. For the electron–water system, the time scale of changes in solvent configurations can be followed by tracking the solvent-induced energetic splitting among the three p-like excited states [29]. On the relatively slow 1–2 ps time scale an electron eventually samples all configurations [17,19]. Hence, we can take the inhomogeneous linewidth to be the average splitting between the highest and lowest p-state, which is ≈ 5875 cm^{-1}.

With knowledge of the lineshape function, the Stokes shift, the solute–solvent coupling and the distribution of solvent sites the results of a variety of three pulse experiments can be calculated [12]. In

Fig. 2a we plot the calculated resonant transient grating signal for the electron assuming (Gaussian) 9 fs pulses, which are short but experimentally attainable. Resonant transient grating spectroscopy is performed in the same experimental configuration as the three-pulse photon echo (detection $-k_1 + k_2 + k_3$), with the exception that there is no time delay between the first two pulses so the experiment probes only population evolution. As illustrated in Fig. 2a, this experiment has the capacity to study solvation dynamics on the sub 40 fs time scale which is not cur-
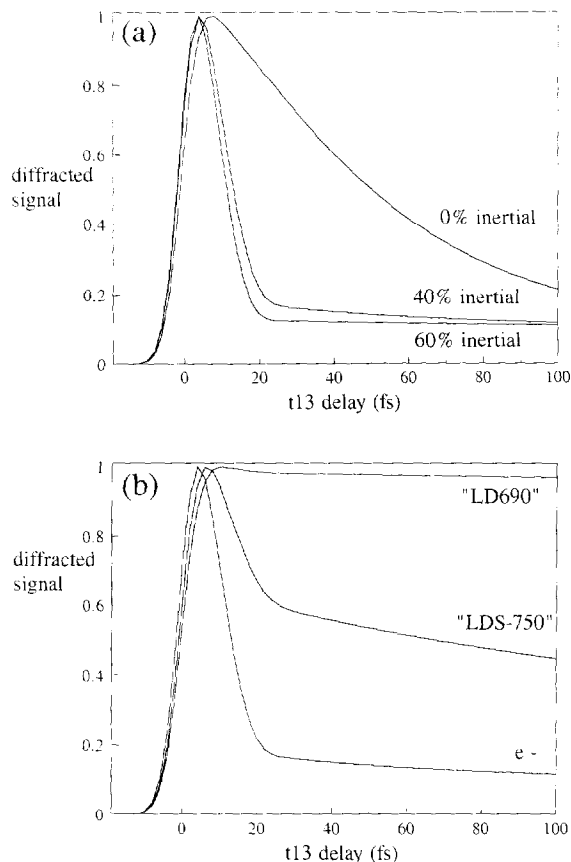

Fig. 2. Calculated resonant transient grating signal assuming 9 fs Gaussian pulses. (a) Signals for the aqueous electron considering different weights of the 20 fs inertial response; the curve labeled 40% corresponds to that observed for the hydrated electron. (b) Calculated signals for hypothetical solutes which have different Stokes shifts, but with the solvent response as that given in Fig. 1. For the electron: $2\lambda = 9600$ cm^{-1}; LDS-750: $2\lambda = 3200$ cm^{-1}; LD690: $2\lambda = 224$ cm^{-1}. The corresponding $\langle [\Delta\omega^2] \rangle$ values as determined by Eq. (4) are $\Delta\omega = 1414$ cm^{-1}, $\Delta\omega = 808$ cm^{-1}, and $\Delta\omega = 215$ cm^{-1}, respectively.

rently accessible using fluorescence upconversion techniques [21]. The inertial contribution to the solvent response can be clearly resolved, while the flat portion of the calculated signal reflects the slower exponential decay in $C(t)$. The MD simulations predict that there is no fast depolarization of the initially excited state and that the lifetime is long compared to the inertial solvation dynamics [17–19]. Hence, these possible decay mechanisms have not been included. The rapid decay in the diffracted signal thus arises solely from the time-dependent shift in the energy gap caused by solvation (the dynamic Stokes shift). The sensitivity of this experiment to the time scale of the solvent response is also shown in Fig. 2a, which displays calculated results for both a solvent response function with a larger inertial contribution and one without an inertial contribution in which $C(t)$ decays exponentially with a 250 fs time constant. In order for this experiment to be sensitive to the solvent fluctuations, however, the probe must have a large enough Stokes shift such that the initially created population moves out of the frequency window probed by the third pulse. Fig. 2b highlights this point by comparing calculated signals for the electron, a time-resolved fluorescence probe LDS-750 [20], and a molecule which has been used in photon echo measurements, LD690 [3,4]. For these probes, the magnitude of the Stokes shift decreases markedly in the order given. In these calculations, $C(t)$ is as given in Fig. 1 and nuclear vibrational motion of the molecular solutes, which can complicate the extraction of solvent information from this experiment [30], is ignored. (The inhomogeneous linewidth is assumed to be 200 cm^{-1} for the dye molecule calculations.)

The calculated three-pulse photon echo signal for the solvated electron is shown as the solid line in Fig. 3a. In this calculation the third pulse is positioned at 100 fs and the second pulse is scanned. The signal is slightly asymmetric, owing to solvent structural changes (transitions between inhomogeneous sites) which are slow compared to the time scale of the decay of the echo [7]. The echo is peaked a few femtoseconds after $t=0$ and decays four orders of magnitude in 15 fs. To understand the origin of this extremely fast dephasing we have also calculated echo signals for a hypothetical solvent response function which contains a larger inertial component and no
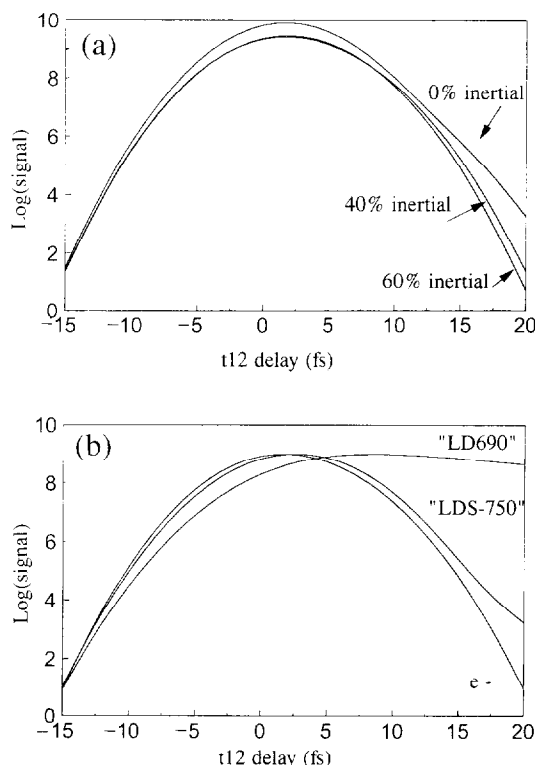

Fig. 3. Log of the calculated photon echo signals assuming 9 fs Gaussian pulses. The delay between the first two pulses is scanned and the third pulse is positioned at 100 fs. (a) Calculated echo signals for the hydrated electron. Central curve: Signal for $C(t)$ as given in Fig. 1. Bottom curve: The inertial contribution is increased to 60% of the total response. Upper curve: the inertial contribution is removed and $C(t)$ decays exponentially with a time constant of 250 fs. (b) Calculated echo signals for different solute Stokes shifts and corresponding $\langle [\Delta\omega^2] \rangle$ as determined by Eq. (4). Electron: $2\lambda = 9660$ cm^{-1}, $\Delta\omega = 1414$ cm^{-1}; LDS-750: $2\lambda = 3200$ cm^{-1}, $\Delta\omega = 808$ cm^{-1}; LD690: $2\lambda = 224$ cm^{-1}, $\Delta\omega = 215$ cm^{-1}. $C(t)$ is given by Fig. 1.

inertial component. Even if the inertial response is removed and the solvent correlation time is 250 fs, the dephasing of the electronic coherence is still extremely fast. The reason for this is illustrated by the calculations shown in Fig. 3b (which are summarized in Fig. 4). Here we use the response function for water determined by the MD simulations (Fig. 1) and consider solutes with different Stokes shifts and thus, by Eq. (4), different degrees of solvent–solute coupling $\langle [\Delta\omega^2] \rangle$. When the solute parameters approach those expected for a molecular system with a change in charge distribution upon excitation,
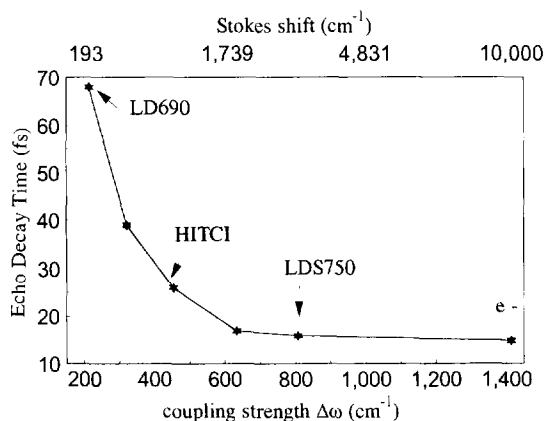
Fig. 4. Plot of the time it takes the calculated echo to decay four orders of magnitude as a function of coupling parameter $\langle [\Delta\omega^2] \rangle$. The upper axis shows the Stokes shift as related by Eq. (4). The solvent response is given by $C(t)$ in Fig. 1. This plot represents solvent effects only; the effects of intramolecular vibrations have not been considered for the molecular solutes (see text).

for example the dye molecule LDS-750 [20], the dephasing of the electronic coherence begins to slow. The dynamics underlying the dephasing in the electron–water system are thus different than that of previously studied molecular systems, where it has been shown that both inertial solvent motion and the solvent–solute coupling are reflected in the decay of the echo [4,5,15,16,31]. In the case of the electron, the dephasing is sensitive only to the magnitude of the electron–water interaction, as given by the coupling parameter $\langle [\Delta\omega^2] \rangle$. Even if the solvent response is quite slow (e.g. no inertial component), small changes in the solvent configuration cause large fluctuations in the transition frequency and thus a loss of coherence [2]. This trade off in the rate of dephasing between inertial solvent dynamics and coupling strength is emphasized in Fig. 4, which makes several predictions for echo measurements with different

solute/solvent combinations [3]. For solutes with large Stokes shifts, the dephasing times will be insensitive to inertial solvent motion. The dephasing time will be solvent sensitive through the solvent–solute coupling as measured by the solvent-dependent Stokes shift. For solutes with small Stokes shifts, the dephasing times will be sensitive to inertial solvent motion, as has been recently demonstrated [4,5]. In this latter case, a solvent dependence should arise primarily because of changes in the time scale of inertial solvent motion. Although the electron–water case is an extreme example of strong solvent–solute coupling, the result that ultrafast dephasing occurs faster than the time scale implied only by inertial solvent dynamics will be general to all systems which undergo substantial changes in charge distribution upon excitation. Experiments exploring these predictions are currently underway [30].

Note added

We note that de Boeij et al. [34] have recently employed an inertial plus diffusive lineshape function to describe their photon echo results of HITCI in ethylene glycol, and Cong et al. [35] have also studied the electronic dephasing of HITCI in ethylene glycol by analyzing the 'coherent artifact' observed in transient absorption data. The solvent–solute coupling for

---

[2] The *first* solvent motions lead to the dephasing of the electronic coherence (due to the large coupling strength). These motions are unquestionably inertial, thus in this limited sense inertial solvent motion causes the dephasing. However, as seen in Fig. 3a, there could be rapid dephasing in absence of inertial motion (again due to the enormous electron–water coupling strength). Thus we conclude the dephasing is dominated by the coupling strength (unlike previously studied systems) and the echo in this case is insensitive to the timescale of the solvent dynamics.

[3] While a Kubo description ($a=0$ in Eq. (5)) is a physically unacceptable model for a liquid with inertial dynamics, we note that Kubo [32] showed that in the limit of rapid fluctuations the dephasing time is a decreasing function of coupling strength, $T_2 = [\tau_{exp} \langle [\Delta\omega^2] \rangle]^{-1}$.

this system is ≈ 416 cm^{-1}, thus, HITCI borders the regime where the echo decay becomes insensitive to the timescale of solvent dynamics and is dominated by the solvent–solute coupling (Fig. 4).

References

[1] P.C. Becker, H.L. Fragnito, J.-Y. Bigot, C. Brito-Cruz, R.W. Schoenlein and C.V. Shank, Phys. Rev. Letters 63 (1989) 505.

[2] J.-Y. Bigot, M.T. Portella, R.W. Schoenlein, C.J. Bardeen, A. Migus and C.V. Shank, Phys. Rev. Letters 66 (1991) 1138.

[3] C.J. Bardeen and C.V. Shank, Chem. Phys. Letters 203 (1993) 535.

[4] C.J. Bardeen and C.V. Shank, Chem. Phys. Letters 226 (1994) 310.

[5] E.T. Nibbering, D.A. Wiersma and K.D. Duppen, Phys. Rev. Letters 66 (1991) 2464.

[6] M. Cho and G.R. Fleming, J. Phys. Chem. 98 (1994) 3478.

[7] A.M. Weiner, S. De Silverstri and E.P. Ippen, J. Opt. Soc. Am. B 2 (1985) 654.

[8] R.F. Loring and S. Mukamel, Chem. Phys. Letters 114 (1985) 426.

[9] S. Mukamel and R.F. Loring, J. Opt. Soc. Am. B 3 (1986) 595.

[10] Y.J. Yan and S. Mukamel, J. Chem. Phys. 89 (1988) 5160.

[11] Y.J. Yan and S. Mukamel, Phys. Rev. A 41 (1990) 6485.

[12] Y.J. Yan and S. Mukamel, J. Chem. Phys. 94 (1991) 179.

[13] M. Maroncelli and G.R. Fleming, J. Chem. Phys. 89 (1988) 5044.

[14] M. Maroncelli, J. Chem. Phys. 94 (1991) 2084.

[15] N.E. Shemetulskis and R.F. Loring, J. Chem. Phys. 97 (1992) 1217.

[16] M. Cho and G.R. Fleming, J. Chem. Phys. 98 (1993) 2848.

[17] B.J. Schwartz and P.J. Rossky, Phys. Rev. Letters 72 (1994) 3282.

[18] B.J. Schwartz and P.J. Rossky, J. Phys. Chem. 98 (1994) 4489.

[19] B.J. Schwartz and P.J. Rossky, J. Chem. Phys. 101, No. 8 (1994), in press.

[20] S.J. Rosenthal, X. Xie, M. Du and G.R. Fleming, J. Chem. Phys. 95 (1991) 4715.

[21] S.J. Rosenthal, N.F. Scherer, M. Cho, X. Xie, M.E. Schmidt and G.R. Fleming, Ultrafast phenomena VIII, eds. A. Migus, J.L. Martin, G.A. Mourou and A. Zewail (Springer, Berlin, 1993) p. 616.

[22] S.J. Rosenthal, R. Jimenez, G.R. Fleming, K. Papazayan and M. Maroncelli, J. Mol. Liquids, T. Fonseca memorial issue, in press.

[23] R. Jimenez, G.R. Fleming, K. Papazayan and M. Maroncelli, Nature 369 (1994) 471.

[24] J.T. Hynes, E.A. Carter, G. Ciccotti, H.J. Kim, D.A. Zichi, M. Ferario and R. Kapral, in: Perspectives in photosynthesis, eds. J. Jortner and B. Pullman (Kluwer, Dordrecht, 1990) p. 133.

[25] E. Carter and J.T. Hynes, J. Chem. Phys. 94 (1991) 5961.

[26] M. Bruehl and J.T. Hynes, J. Phys. Chem. 96 (1992) 4068.

[27] J.T. Hynes, Chem. Phys. 176 (1993) 521.

[28] R.M. Stratt and M. Cho, J. Chem. Phys. 100 (1994) 6700.

[29] P.J. Rossky and J. Schnitker, J. Phys. Chem. 92 (1988) 4277.

[30] S.J. Rosenthal, C.J. Bardeen and C.V. Shank, in preparation.

[31] A.M. Walsh and R.F. Loring, Chem. Phys. Letters 186 (1991) 77.

[32] R. Kubo, Advan. Chem. Phys. 15 (1969) 101.

[33] W.T. Pollard, S.L. Dexheimer, Q. Wang, L.A. Peteanu, C.V. Shank and R.A. Mathier, J. Phys. Chem. 96 (1992) 6147.

[34] W.P. de Boeij, M.S. Pshenichnikov, K. Duppen and D.A. Wiersma, Chem. Phys. Letters 224 (1994) 243.

[35] P. Cong, Y.J. Yan, H. Deuel and J.D. Simon, J. Chem. Phys. 100 (1994) 7855.